Effect of coalescence energy release on the temporal shape evolution of nanoparticles

Kari E. J. Lehtinen* and Michael R. Zachariah†

Department of Mechanical Engineering and Department of Chemistry, University of Minnesota, Minneapolis, Minnesota 55455

(Received 24 October 2000; published 16 April 2001)

The driving force for coalescence of two nanoparticles is the reduction in free energy through a reduction in surface area. The resulting particle also has a lower total potential energy, which through conservation of energy can lead to a significant increase in particle temperature. In a growth process particle heating competes with heat transfer to the cooler carrier gas. In this paper we develop a model that illustrates that this temperature increase can be extremely important and should be accounted for when modeling collision/coalescence processes. Our calculations indicate that the heat release associated with particle coalescence may reduce the coalescence time by as much as a few orders of magnitude. This is especially true for the final stages of exponential surface area decay toward sphericity, which becomes much faster and qualitatively explains the fact that primary particles of only a few nanometers in diameter are of spherical shape. We develop in this analysis a dimensionless ''coalescence heating number,'' which can be used to assess if the exothermic nature of coalescence should be accounted for under a given set of conditions. We also show that a simple coalescence model, which includes the temperature effect, closely follows our prior molecular dynamics calculations for silicon nanoparticles sintering. This analysis also explains a set of experimental results for alumina nanoparticle production, previously unexplainable by classical methods. Finally, we see that lower gas pressures result in lower gas-phase heat transfer, which in turn results in larger primary particles.

INTRODUCTION

The ability to predict and control the primary particle size of nanostructured materials is essential since it is a key variable in many thermal, mechanical, and optical properties.[1] Typically in many industrial aerosol processes, a high concentration of very small particles undergoes rapid coagulation. This may lead to the formation of fractal-like agglomerates consisting of a large number of spheroidal primary particles of approximately uniform diameter.[2] The size of the primary particles ultimately is determined by the rates of collision and coalescence.[3] At high temperatures, coalescence occurs almost on contact, resulting in large primary particles and hence small surface area. At low temperatures, the collision rate is faster than the rate of coalescence, leading to fractal-like agglomerates consisting of very small primary particles and thus large surface area. Controlling the coalescence rate is possible through knowledge of the material properties and the time temperature history of the reactor, and the collision rate through the volume loading of the material.[4]

Ulrich and Subramanian[5] first described simultaneous collision and coalescence of agglomerates in flames by assuming that agglomerates consist of a large number of primary particles and treating collision and coalescence as separable processes. Koch and Friedlander[6] assumed that the coalescence rate of an agglomerate is directly proportional to its excess surface area [(actual surface area)−(equivalent spherical area)]. This was later shown by Friedlander and Wu[7] to be exact for the final stages of transformation to sphericity for an originally slightly nonspherical particle. This simple linear decay law for the agglomerate surface area, when combined with a method for solution of the aerosol dynamic equation, has resulted in several successful models for particle size prediction.[8–12] However, in some cases, particularly those that predict very small primary particles of only a few nanometers, these models seem to break down[10,13,14] and underpredict the primary particle size.

Ehrman[15] suggested that one reason for this might be a very high internal pressure of particles under approximately 5 nm in diameter. Based on some of our recent molecular dynamics simulations[16] we believe this will not completely explain this effect.

This study was primarily motivated by the results of Zachariah and Carrier,[17] who studied the coalescence of silicon nanoparticles using molecular dynamics (MD) simulation methods. They found that when two particles coalesce the formation of new chemical bonds results in energy release, and therefore a significant increase in particle temperature. This is illustrated in Fig. 1, in which particle temperature vs time is shown for a typical coalescence event. Following a collision the formation of new chemical bonds between the particles results in heat release and the formation of a neck between the particles. In turn this results in further energy release which increases the particle temperature rapidly and thus also speeds up the coalescence. An oval shape is formed, which then slowly evolves into a sphere.

Since these particles coalesce by the mechanism of solid state diffusion, which is an extremely sensitive function of temperature, we expect any temperature increase within the particle to have an important effect on the dynamics of coalescence. In this paper we demonstrate how the heat release resulting from coalescence can be straightforwardly incorporated into a Koch and Friedlander[6] type of coalescence model. In particular, our aim is to highlight the sharp transition for conditions in which the heat release plays a significant role in the dynamics of particle coalescence.
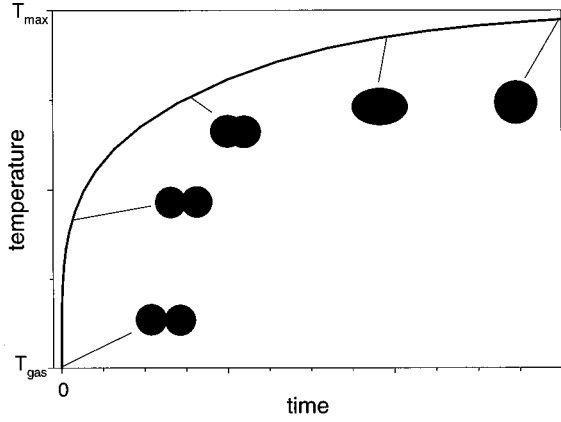
FIG. 1. The evolution of particle temperature and shape in nanoparticle coalescence. The decreasing surface area results in an energy release and thus an increase in temperature.

THEORY

We begin our analysis by considering a system consisting of two identical spherical particles each with N atoms. During coalescence, a neck rapidly forms between the particles, which transforms into a spherule and slowly approaches a sphere (see Fig. 1 of this paper or Fig. 3 of Ref. 18). We assume that the energy E of our system throughout the coalescence process can be described with bulk and surface contribution terms[17]

$$E = E_{bulk} + E_{surf},$$

$$E_{bulk} = 2N[\epsilon_b(0) + c_v T_p], \quad (1)$$

$$E_{surf} = \sigma a,$$

where a is the surface area of the coalescing pair of particles, σ the surface tension, $\epsilon_b(0)$ the bulk binding energy (negative) at zero temperature, and c_v the constant-volume heat capacity. Any change in total energy of the particle can only result from energy loss to the surroundings. Neglecting any radiation heat transfer effects, the change in particle energy is equal to the cooling rate arising from collisions with bath gas molecules (rate Z):

$$\frac{dE}{dt} = 2Nc_v \frac{dT_p}{dt} + \sigma \frac{da}{dt} = -Zc_g(T_p - T). \quad (2)$$

Here T is the gas temperature and c_g the heat capacity of the gas molecules. By rearranging and assuming that the surface area reduction can be approximated by the well-known linear rate law developed by Koch and Friedlander[6]

$$\frac{da}{dt} = -\frac{1}{\tau_f}(a - a_{sph}), \quad (3)$$

we get

$$2c_v N \frac{dT_p}{dt} = \frac{\sigma}{\tau_f}(a - a_{sph}) - Zc_g(T_p - T), \quad (4)$$

where the characteristic coalescence or fusion time (for volume diffusion) is

$$\tau_f = \frac{3kTN}{64\pi\sigma D} \quad (5)$$

and

$$Z = \frac{p a_{sph}}{\sqrt{2\pi m_g kT}} \quad (6)$$

is the collision rate of the free molecular particle with gas molecules (of mass m), obtained from kinetic gas theory. The sensitivity to temperature comes from the exponential dependence of the diffusion coefficient D on temperature:

$$D = A \exp\left(-\frac{B}{T_p}\right). \quad (7)$$

Now, in Eq. (4), the first term on the right-hand side (RHS) is the heat increase due to coalescence, as explained earlier. The second term on the RHS is the heat loss due to collisions with gas molecules. The collision rate Z of the free molecular particle with gas molecules (of mass m) is assumed to be unaffected by the coalescence shape evolution.

A convenient nondimensionalization of Eq. (5) can be obtained through

$$t^* = \frac{t}{\tau_0}, \quad T^* = \frac{T_p - T}{T}, \quad a^* = \frac{a - a_{sph}}{a_{sph}}, \quad (8)$$

resulting in

$$\frac{dT^*}{dt^*} = \frac{E_s}{E_b}\frac{\tau_0}{\tau}a^* - \frac{E_g}{E_b}T^* \quad (9)$$

and

$$\frac{da^*}{dt^*} = -\frac{\tau_0}{\tau}a^*. \quad (10)$$

Here $E_s = \sigma a_{sph}$, $E_b = 2c_p NT$, $E_g = \tau_0 Z c_g T$, and τ_0 is the coalescence time calculated at the gas temperature T. Equations (9) and (10) are straightforward to integrate numerically, and we did so for several sets of system parameters for silicon and alumina.

A simple criterion to estimate the importance of coalescence-induced heating would naturally be useful. In the Appendix, Eq. (9) is solved approximately, resulting in a dimensionless quantity, the coalescence heat increase number H:

$$H = \exp\left(\frac{B}{T_g}\frac{T_{max}}{T_{max}+1}\right) \Big/ (T_{max}+1),$$

$$T_{max} = \frac{E_s A_0^*}{E_b - E_g}\left[\exp\left(\frac{E_g \ln(E_g/E_b)}{E_b - E_g}\right) - \exp\left(\frac{E_b \ln(E_g/E_b)}{E_b - E_g}\right)\right]. \quad (11)$$

Physically, H is an enhancement in the coalescence rate:

TABLE I. Comparison of maximum temperature and coalescence time for Si nanoparticles at $T=600$ K from this work with the MD results of Zachariah and Carrier (Ref. 18).

N	ΔT (MD) (K)	τ (MD) (ps)	ΔT (K)	τ (ps)
30	486	130	580	320
60	402	600	460	860
120	386	1700	365	2300
240	313	2500	290	6070

$$H \approx \frac{\tau_0 - \tau}{\tau},\tag{12}$$

where the approximation holds for small temperature increases. Even if H cannot be used to accurately predict the actual coalescence enhancement for cases with significant heat release, it is useful as an indicator for determining if the heating effect is important, as will be shown in the next section.

RESULTS AND DISCUSSION

We began by repeating the solid state cases of Zachariah and Carrier,[18] i.e., we simulated the coalescence of silicon nanoparticles of size $N=30$, 60, 120, and 240 for gas temperature $T=600$ K, using the same material properties. The results are summarized in Table I.

The fact that the maximum temperatures agree quite well shows that the use of the energy formulation of Eq. (1) is reasonable. In Table I the coalescence time is defined as the time for 95% decrease in excess surface area (compared with the completely coalesced perfect sphere). It must be noted that in the MD simulations of Zachariah and Carrier[18] the coalescence time was extracted from the time evolution of the moments of inertia of the coalescing particles.

To assess the competing effects of heat release and bath gas cooling, silicon particle coalescence was simulated for $N=100$, 1000, and 10 000 at $T_g=600$ K, as well as for $N=1000$ at $T_g=400$ K. The calculations were conducted with and without the heat release effect and are presented in Figs. 2(a)–2(d). The dashed line in each case corresponds to a calculation in which the heat release due to coalescence has been neglected. The solid line and dotted line are the excess
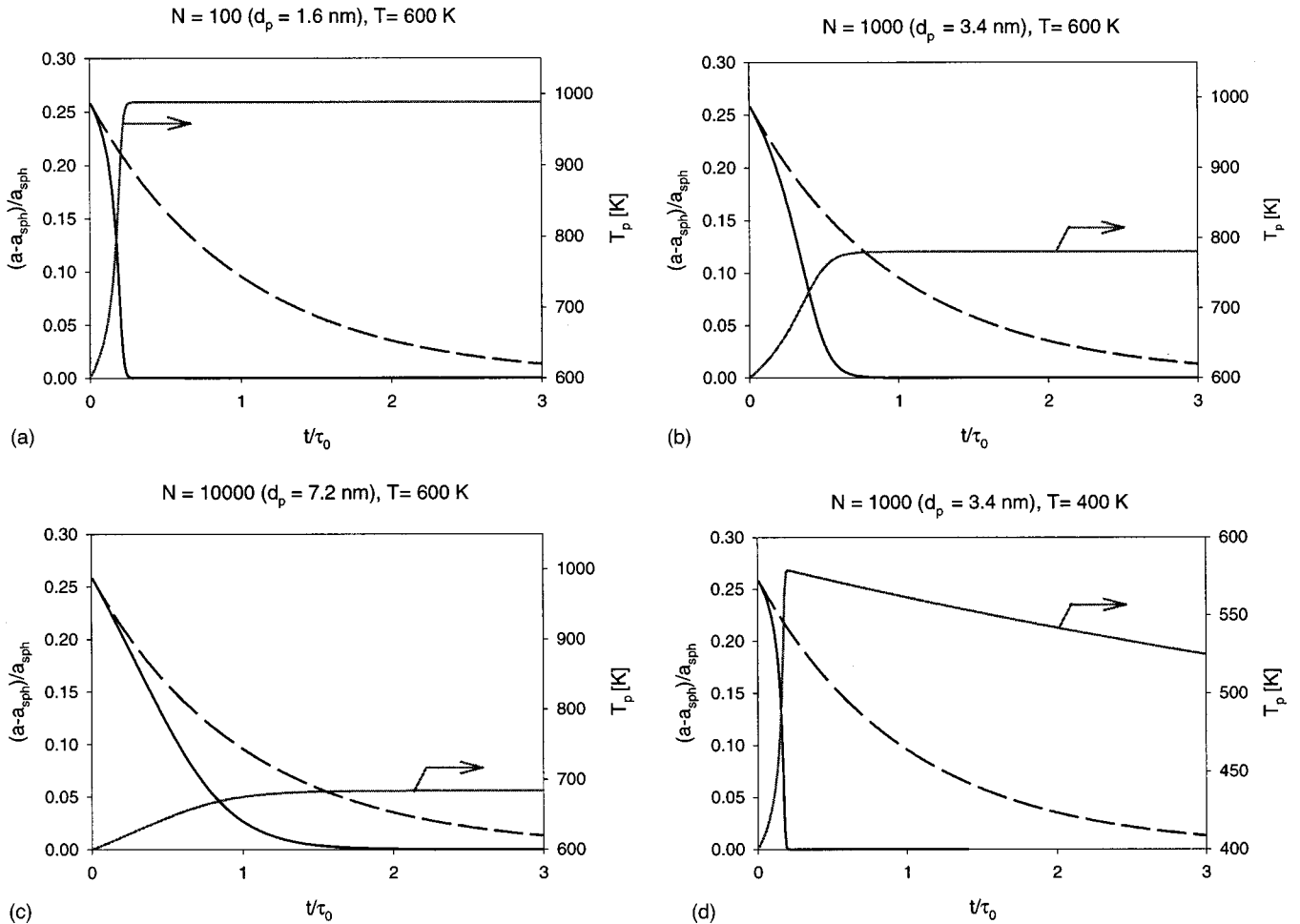
FIG. 2. The evolution of surface area (solid line) and temperature (gray line) of coalescing silicon nanoparticles at $T_g=600$ K of size $N=$(a)100, (b) 1000, and (c) 10 000 atoms, and (d) at $T_g=400$ K of size $N=1000$ atoms. The dashed line is the surface area evolution if coalescence heat release is neglected.

$\tau_f (T_g)$ for a particle of 100 Si atoms

(a)

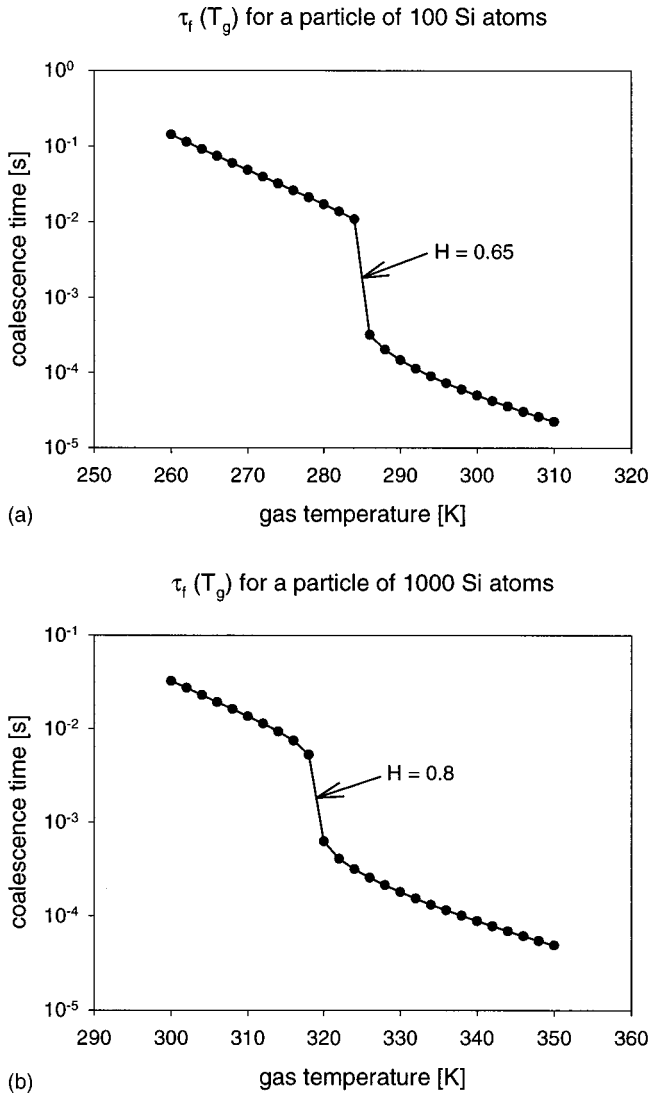$\tau_f (T_g)$ for a particle of 1000 Si atoms

(b)

FIG. 3. The coalescence time of silicon nanoparticles of size $N=100$ and 1000 atoms as a function of gas temperature. The sudden changes occur at the values $H=0.65$ and 0.8.

surface area and the particle temperature from the numerical solution to Eqs. (9) and (10), i.e., the heat release and gas cooling are accounted for.

It is evident that the heat release has a strong effect on the coalescence dynamics. If the conditions are favorable for neck formation, i.e., the temperature is high enough, the particle temperature starts to increase, which in turn feeds back to increase the rate of coalescence. The final stages of coalescence to a sphere, which typically take a long time compared with the initial neck formation, occur much more quickly in these cases. This effect is particularly important for very small particles, of a few nanometers in diameter, which show a much slower coalescence rate when neglecting heat release effects. From a practical standpoint, for example, when gases in a reactor are cooling, one would expect to see agglomerates consisting of primary particles that are not spherical since the transition from oval to sphere in the absence of heat release is by far the slowest process. However, nanosized primary particles are observed to be spheri-

cal, and we believe the heat release from coalescence is a possible explanation for this.

We see in Figs. 2(a)–2(c) that for the gas temperature of 600 K the coalescence is sufficiently fast that heat conduction to the surrounding gas is negligible, as evidenced by the flat temperature profile during the neck growth process. At 400 K [Fig. 2(d)]. However, cooling is clearly seen to have an effect, although in this case at least cooling takes place well after the spherical shape is obtained, around $t/\tau_0 = 0.2$.

To illustrate the sensitivity of the dynamics of Eq. (9) [or Eq. (4)] to temperature, we plotted the coalescence time as a function of gas temperature. Presented in Figs. 3(a) and 3(b) we see that for particles with 100 and 1000 atoms there exists a temperature at which there is a sudden change in the dynamics of Eq. 9. Figure 3(a) shows that below the critical temperature particle heating is negligible and the coalescence time is long. Then, over a very narrow temperature window at around 285 K the coalescence time drops two orders of magnitude for the $N=100$ case and an order of magnitude for $N=1000$. This clearly illustrates the nonlinear nature of the competing heat generation/extraction terms. If a critical temperature increase is exceeded, it increases the coalescence rate exponentially, which correspondingly speeds up the temperature increase rate, and so on. If this critical temperature is not exceeded, coalescence is slow and the heat release energy is conducted to the surrounding gas.

Moreover, this sudden change seems to occur at roughly the same value for the heating number, in the range $H = 0.6–0.9$. As explained in the previous section, the heating number is an approximation to the coalescence rate increase. If the value for H is small, say under 0.5, than coalescence rate increase arising from heat release is essentially negligible. If it exceeds 1, then the coalescence rate increase is significant and must be taken into account in any modeling effort. Between these values, at around 0.6–0.9, there is a sudden change in coalescence dynamics, a narrow window of conditions in which the heat release triggers very fast coalescence. In other words, we can conclude that if the heating number is above this critical value particle heating resulting from energy release should be accounted for in the computation of the coalescence time. For example, for the cases presented in Figs. 2(a)–2(d), the heating number H has the values 84.8 (a), 13.1 (b), 3.1 (c), and 83.4 (d), which means that coalescence heat release is important in all those cases.

Figure 4 presents results in which we compute the coalescence time as a function of particle size for a specified gas temperature. In the absence of heating effects we expect the coalescence time to increase linearly with the number of atoms, based on the solid state diffusion model. Instead we see a clear transition from a rapid coalescence regime to a slow one at around 1700 atoms, corresponding again to a heating number of 0.9.

Since the sharp transition occurs at a nearly constant value for H, it can be used to identify the regions in particle-size–temperature space in which the heat release is important. In Fig. 5 the equation $H=0.8$ (solid line) is plotted in size-temperature space. The curves represent the gas temperature at which a given particle size will have a heating effect. Alternatively, one can view this curve as representing

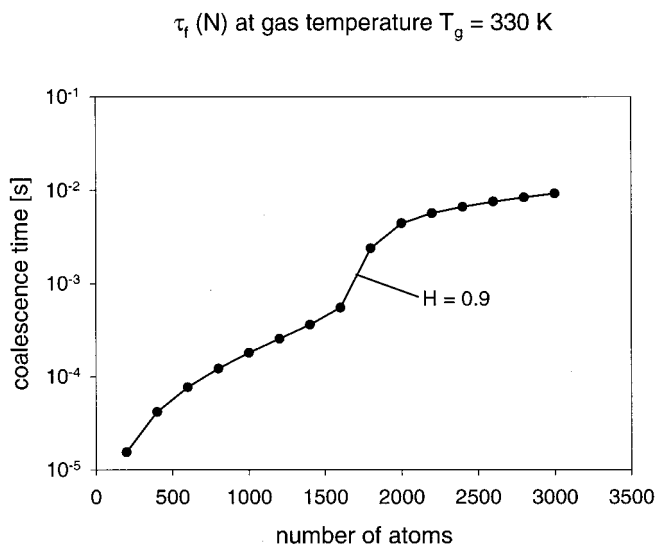τ_f (N) at gas temperature T_g = 330 K

FIG. 4. The coalescence time of silicon nanoparticles of variable size at gas temperature $T_g = 330$ K. The sudden change occurs at the value $H = 0.9$.

a temperature for which all particles smaller than the critical particle will undergo self-heating. The dotted lines are curves for $H = 0.6$ and 1.0 and indicate that the demarcation is not sensitive in this range of H values.

Since the cooling rate is proportional to gas pressure, this analysis also provides a tool for primary particle size control. In Fig. 6 we have repeated the solution of the nonlinear equation $H = 0.8$, but with different values for the bath gas pressure. It is evident that for a given gas temperature the sharp transition from fast to slow coalescence occurs at larger particle sizes for a lower pressure. Thus a lower-pressure growth condition should enhance the ability to produce larger primary particles of spherical shape. This is an intriguing aspect when one considers that total gas pressure,
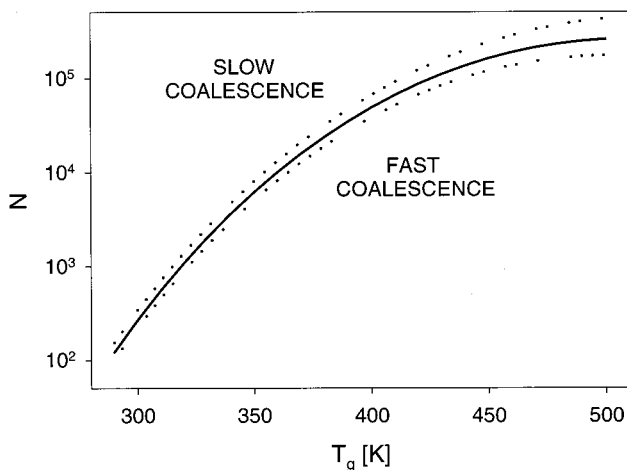

FIG. 5. The size vs temperature for $H = 0.8$ (solid line), i.e., the location of the sudden change in coalescence time. Above the curve, heating due to coalescence does not affect the coalescence rate, while below the effect is significant. The dotted lines are for $H = 0.6$ and 1.0.
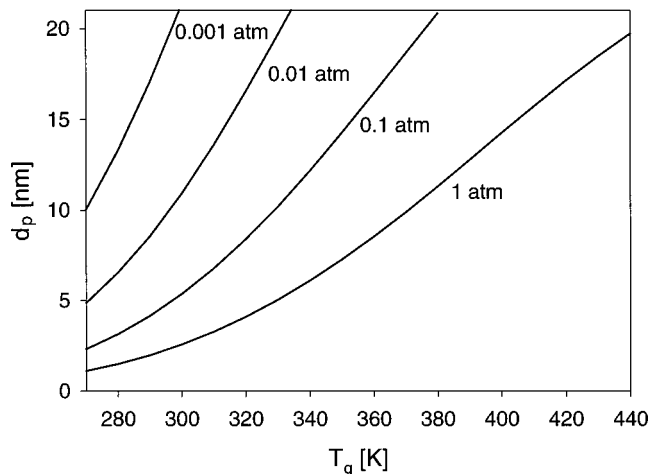

FIG. 6. Effect of pressure on the location of the sudden change in coalescence time, i.e., solution to the equation $H = 0.8$ in particle size vs temperature.

to our knowledge, has never been considered a control variable for primary particle size. We are currently in the process of further investigating this behavior.

The results presented so far are for silicon where we have molecular dynamics simulation results. We now apply this model to alumina nanoparticle growth, and in particular to the experimental results of Windeler *et al.*[10] These experiments are of interest because of the controlled nature of the growth conditions and the fact that the standard Koch and Friedlander[6] model failed to produce any significant particle growth. Indeed, this lack of agreement was first encountered in experiments of Wu *et al.*[13] Reference 10 involved a free jet injection of trimethyl aluminum vapor reacting in a methane-air flame forming alumina nanoparticles. The primary particles produced were of volume mean diameter 4.1, 6.8, and 10.7 nm for (maximum) flame temperatures of 1700, 1800, and 1900 K, respectively. These experimental data, along with the $H = 0.8$ curve for alumina, are presented in Fig. 7. The experimental points seem to match the $H = 0.8$
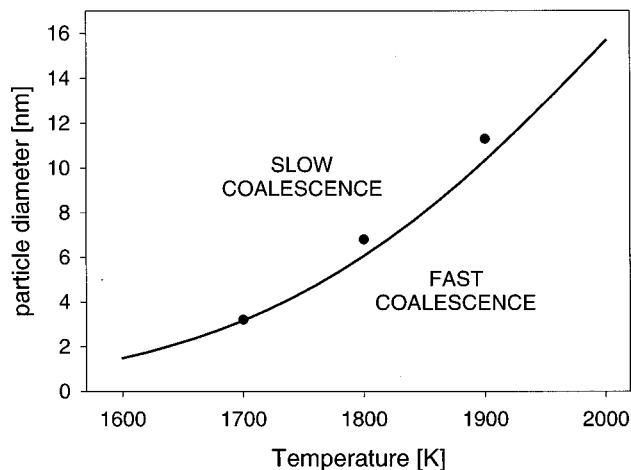

FIG. 7. The size-temperature curve representing the solution for $H = 0.8$ for alumina, i.e., the location of the sudden change in coalescence time. The dots represent experimental results from Ref. 10.

curve very well. What we believe happens is as follows. In the hot flame the particles start growing from molecular size by coagulation. They coalesce as they collide, aided by the heat release from coalescence, up to the point where the sudden drop in coalescence rate occurs. The location of this sudden drop is indicated by the $H=0.8$ curve in Fig. 7. Thereafter, each collision just increases the number of primary particles per agglomerate, and the primary particle size is frozen.

CONCLUSIONS

In this paper, we have presented an analysis of the thermal behavior of coalescing nanoparticles. We include the effects of energy release during coalescence, which to our knowledge has not been accounted for in previous collision-coalescence modeling. The driving force for the transformation of two spherical nanoparticles into one completely fused particle is a minimization of the surface free energy and is reflected in a temperature increase of the resulting particle. Since the characteristic coalescence time is inversely proportional to the solid state diffusion coefficient, which is very sensitive (exponentially dependent) to temperature, the heat release associated with the initial stages of coalescence (under certain circumstances) can significantly impact the overall coalescence process. In this study, we have used a simple exponential decay law for the excess surface area of the coalescing particles, and modified it in such a way that particle temperature and hence also the characteristic coalescence time are time-dependent variables.

We have used this formulation to calculate the coalescence of silicon and alumina nanoparticles. Coalescence heat release can result in particle temperatures several hundred degrees hotter than the carrier gas, which can, through an increase in the diffusion coefficient, increase the coalescence rate by 1–3 orders of magnitude. This effect is significant for small particles especially, since their fraction of surface atoms is largest and their overall heat capacity small, relative to larger particles. Larger particles, which have a low sintering rate and a higher heat capacity, result in low heating as sufficient time exists for bath gas heat transfer to maintain the particle at isothermal conditions. We have investigated the behavior under a variety of particle sizes and bath gas temperatures and have determined that there exists a very sharp transition. The highly nonlinear nature of the model indicates that the coalescence time can drop by orders of magnitude for a few degrees increase in temperature.

A dimensionless number, the coalescence heating number H, has been derived in order to analytically determine if particle heating is important. The above-mentioned sharp transition seems to occur at $H=0.6-0.9$ for various condi-

tions of silicon and alumina nanoparticle coalescence. Solving for the temperature and particle size from the equation $H=$ const gives the transition curve in temperature-size space.

Since the exponential decay from an oval shape to a perfect sphere is a slow process, one would expect to see under typical experimental conditions mainly nonspherical primary particles in agglomerates. This is not the case, however, particularly when the primary particles are small (a few nanometers in diameter); they are typically all spherical. The enhanced coalescence rate resulting from heat release greatly shortens the relative time for the final stages of shape evolution and thus favors the freezing out of spherical particles. Furthermore, we repeated the analysis using different values for the total gas pressure. The sharp transition from fast to slow coalescence, at a given gas temperature, occurs at larger particle sizes when using a lower gas pressure. Thus a lower pressure can be used if larger spherical primary particles are desired.

APPENDIX

Let us study a simplified version of Eq. (10), namely,

$$\frac{dT}{dt} = ha_0 e^{-t} - cT. \tag{A1}$$

This is exactly the same as Eq. (10), with $h=E_s/E_b$ and $c=E_g/E_b$, except that τ_0/τ is assumed to be 1 and a is assumed to decay as $a=a_0 \exp(-t)$. The solution to Eq. (A1) is

$$T = \frac{ha_0}{1-c}(e^{-ct} - e^{-t}). \tag{A2}$$

The maximum of this function

$$T_{\max} = \frac{ha_0}{1-c}\left[\exp\left(\frac{c \ln c}{1-c}\right) - \exp\left(\frac{\ln c}{1-c}\right)\right], \tag{A3}$$

is now an approximation to the maximum particle temperature achieved during coalescence. The importance of this temperature results from the fact that for any thermally activated process it is the maximum temperature that determines the temporal behavior and kinetics of the system.

We now define the heating number H to be the coalescence rate increase $(\tau_0 - \tau)/\tau$ using this maximum temperature from Eq. (A3):

$$H = \frac{\tau_0 - \tau}{\tau} = \exp\left(\frac{B}{T_g}\frac{T_{\max}}{T_{\max}+1}\right) \Big/ (T_{\max}+1) - 1. \tag{A4}$$

*On leave from VTT Energy, P.O. Box 1401, 02044 VTT, Finland. Electronic address: kari.lehtinen@vtt.fi

†Author to whom correspondence should be addressed. Electronic address: mrz@me.umn.edu

[1] N. Ichinose, Y. Ozaki, and S. Kashu, *Superfine Particle Technology* (Springer-Verlag, Berlin, 1992).

[2] C. M. Megaridis and R. A. Dobbins, Combust. Sci. Technol. **71**, 95 (1990).

[3] K. E. J. Lehtinen, R. S. Windeler, and S. K. Friedlander, J. Aerosol Sci. **27**, 883 (1996).

[4] S. E. Pratsinis, Prog. Energy Combust. Sci. **24**, 197 (1998).

[5] G. D. Ulrich and N. S. Subramanian, Combust. Sci. Technol. **17**,

119 (1977).

[6] W. Koch and S. K. Friedlander, J. Colloid Interface Sci. **140**, 419 (1990).

[7] S. K. Friedlander and M. K. Wu, Phys. Rev. B **49**, 3622 (1994).

[8] Y. Xiong and S. E. Pratsinis, J. Aerosol Sci. **24**, 283 (1993).

[9] F. E. Kruis, K. A. Kusters, S. E. Pratsinis, and B. Scarlett, Aerosol. Sci. Technol. **19**, 514 (1993).

[10] R. S. Windeler, S. K. Friedlander, and K. E. J. Lehtinen, Aerosol. Sci. Technol. **27**, 191 (1997).

[11] M. Shimada, T. Seto, and K. Okuyama, J. Chem. Eng. Jpn. **27**, 795 (1994).

[12] T. Johannesen, Ph.D. thesis, TU Denmark, 1999.

[13] M. K. Wu, R. S. Windeler, C. K. R. Steiner, T. Bors, and S. K. Friedlander, Aerosol. Sci. Technol. **19**, 527 (1993).

[14] S. H. Ehrman, S. K. Friedlander, and M. R. Zachariah, J. Aerosol Sci. **29**, 687 (1998).

[15] S. H. Ehrman, J. Colloid Interface Sci. **213**, 258 (1999).

[16] I. V. Schweigert, K. E. J. Lehtinen, M. J. Carrier, and M. R. Zachariah (unpublished).

[17] M. R. Zachariah, M. J. Carrier, and E. Blasiten-Barojas, J. Phys. Chem. **100**, 14 856 (1996).

[18] M. R. Zachariah and M. J. Carrier, J. Aerosol Sci. **30**, 1139 (1999).